Mutational Analysis of a Ribonuclease III Processing Signal†

Bhadrani Chelladurai, Honglin Li, Kejing Zhang, and Allen W. Nicholson*

Department of Biological Sciences, Wayne State University, Detroit, Michigan 48202

Received December 28, 1992; Revised Manuscript Received April 12, 1993

ABSTRACT: A mutational approach was employed to identify sequence and structural elements in a ribonuclease III processing signal that are important for *in vitro* enzymatic cleavage reactivity and selectivity. The substrate analyzed was the bacteriophage T7 R1.1 processing signal, a 60 nucleotide irregular RNA hairpin exhibiting an upper and lower dsRNA stem, separated by an asymmetric internal loop which contains the scissile phosphodiester bond. Altering the length of either the upper or lower dsRNA segment in R1.1 RNA does not change the site of RNase III cleavage. However, decreasing the size of either the upper or lower dsRNA segment causes a progressive inhibition of processing reactivity. Omitting monovalent salt from the reaction buffer promotes cleavage of otherwise unreactive R1.1 deletion mutants. Accurate processing is maintained with R1.1 variants containing specific point mutations, designed to disrupt Watson–Crick (WC) base-pairing in a conserved sequence element within the upper dsRNA stem. The internal loop is not required for processing reactivity, as RNase III can accurately and efficiently cleave R1.1 variants in which this structure is WC base-paired. Moreover, an additional cleavage site is utilized in these variants, which occurs opposite the canonical site, and is offset by two nucleotides. The fully base-paired R1.1 variants form a stable complex with RNase III in Mg^{2+}-free buffer, which can be detected by a gel electrophoretic mobility shift assay. In contrast, the complex of wild-type R1.1 RNA with RNase III is unstable during nondenaturing gel electrophoresis. Thus, a functional role of the T7 R1.1 internal loop is to enforce single enzymatic cleavage, which occurs at the expense of RNase III binding affinity.

The essential role of protein–RNA interactions in gene expression and regulation has spurred much research on the molecular determinants of specificity in protein recognition of RNA. The study of prokaryotic RNA processing reactions has provided important information on the functional consequences of protein recognition and cleavage of primary transcripts (Gegenheimer & Apirion, 1981; Altman et al., 1982; King et al., 1986; Deutscher, 1988, 1990; Brawerman & Belasco, 1993). Current experimental efforts are directed toward identifying RNA and protein components which provide binding energy, confer specificity, and promote catalysis of RNA processing. In distinction from RNA binding proteins, RNA processing enzymes may be able to discriminate between substrates in the reaction transition state as well as at the substrate binding step.

Ribonuclease III of *Escherichia coli* (RNase III, EC 3.1.24)[1] is a dsRNA-specific endoribonuclease (Dunn, 1982; Robertson, 1982; Court, 1993). RNase III carries out site-specific cleavage of dsRNA-containing structures (processing signals) within cellular, viral, and plasmid-encoded transcripts. RNase III is highly selective, typically catalyzing the hydrolysis of one or two specific phosphodiester bonds within the processing signals. RNase III can alter mRNA translational efficiencies either by cleavage (Saito & Richardson, 1981) or perhaps through binding without cleavage (Altuvia et al., 1987). RNase III processing can also trigger mRNA turnover (Regnier & Grunberg-Manago, 1990), and the translation of the *rnc* (RNase III) cistron is self-regulated through RNase III cleavage-induced destabilization of the *rnc* operon mRNA (Bardwell et al., 1989). The recognition elements which define RNase III processing signals have been the subject of ongoing speculation, with some experimentation (Robertson, 1977; Gegenheimer & Apirion, 1981; Robertson, 1982; Dunn, 1982; Krinke & Wulff, 1990; Chelladurai et al., 1991; Court, 1993). Though required for processing reactivity, the presence of dsRNA *per se* is insufficient to establish selectivity. In particular, the ability of RNase III to nonspecifically degrade dsRNA polymers demands the existence of cleavage specificity determinants within RNase III processing signals. The puzzle of RNase III processing selectivity has been underscored in a study of the reactivity of a 55 bp sense–antisense RNA–RNA duplex of phage lambda, in which specific phosphodiester linkages are cleaved by RNase III while adjacent ones are unreactive (Krinke & Wulff, 1990). A conserved base-paired sequence (CUU/GAA) has been noted near the cleavage sites of a number of RNase III substrates (Bram et al., 1980; Gegenheimer & Apirion, 1981; Steege et al., 1987; Daniels et al., 1988). However, it was recently shown that base pair substitutions within the CUU/GAA element do not affect the selectivity of *in vitro* cleavage of a phage T7 processing signal (Chelladurai et al., 1991). The possible involvement of RNA secondary structure in establishing RNase III processing selectivity has also been considered. Through the comparison of processing signal secondary structures and cleavage site locations, it has been suggested that RNase III may act as a "molecular ruler", measuring 10–13 bp from one end of a dsRNA segment to select the scissile phosphodiester bond(s) (Robertson, 1982; Krinke & Wulff, 1990). This model has not been critically tested.

The bacteriophage T7 R1.1 processing signal[2] is under study in our laboratory as a representative substrate with which to determine RNase III recognition elements (Nicholson et al.,

† Supported by NIH Grant GM41283.

[1] Abbreviations: bp, base pair; dsRNA, double-stranded RNA; nt, nucleotide; TBE, Tris base (89 mM), boric acid (89 mM), EDTA (2 mM); WC, Watson–Crick.

[2] The R1.1 RNase III processing signal is located between the T7 early genes 1 and 1.1 and has been alternatively called the R4 processing signal (Dunn & Studier, 1983; Court, 1993). In this paper, "processing signal" and "processing substrate" are used interchangeably, and "processing site" or "cleavage site" refers to the scissile phosphodiester bond.

0006-2960/93/0432-7549$04.00/0

1988; Chelladurai et al., 1991; Nicholson, 1992). The R1.1 processing signal (Figure 1) is an approximately 60 nt irregular RNA hairpin, formally containing an asymmetric internal loop which separates an upper and a lower dsRNA stem. This secondary structural motif appears to provide a conserved biological function, as it is characteristic of most of the other processing signals in T7 (Dunn & Studier, 1983) and is seen in other viral and cell-encoded RNase III substrates (Pragai & Apirion, 1981; Montanez et al., 1986; Steege et al., 1987; Regnier & Grunberg-Manago, 1990; Faubladier et al., 1990). The R1.1 processing signal is cleaved by RNase III at a single (primary) site *in vivo* (Oakley & Coleman, 1977; Kramer et al., 1977; Rosenberg et al., 1977), as well as *in vitro*, involving either the 7200 nt T7 polycistronic early mRNA precursor (Dunn, 1976) or small transcripts (Nicholson et al., 1988; Chelladurai et al., 1991). We have recently shown that the enzymatic cleavage of R1.1 RNA *in vitro* obeys Michaelis–Menten kinetics (Li et al., 1993), indicating a reaction pathway involving substrate binding to a saturable site, followed by chemical catalysis and product release. We present in this paper a study of the *in vitro* cleavage reactivities and enzyme binding properties of specific variants of the R1.1 processing signal. We evaluate the molecular ruler model for RNase III cleavage site selection and examine the role of the internal loop in the processing reactivity and biological function of an RNase III processing signal.

EXPERIMENTAL PROCEDURES

Materials. Chemicals and reagents used were of the highest quality commercially available. Water was purified by a Millipore MilliQ$^+$ system. The radiolabeled nucleotides [α-^{32}P]UTP (3000 Ci/mmol) and [γ-^{32}P]ATP (3000 Ci/mmol) were from Du Pont–NEN (Boston, MA), while unlabeled rNTPS were from United States Biochemical Corp. (Cleveland, OH) or Pharmacia LKB (Piscataway, NJ). *E. coli* bulk stripped tRNA was from Sigma (St. Louis, MO). DNA oligonucleotides were synthesized by the Wayne State Macromolecular Core Facility or by the Midland Certified Reagent Co. (Midland, TX) and further purified by gel electrophoresis. Calf alkaline phosphatase was from Boehringer-Mannheim (Indianapolis, IN), while T4 polynucleotide kinase was from Promega (Madison, WI). T7 RNA polymerase was purified in-house, using an overexpressing bacterial strain and following the procedure of Grodberg and Dunn (1988). RNase III was purified to homogeneity (Li et al., 1993) from *E. coli* HMS174(DE3) cells, which carried the *rnc* gene cloned in the plasmid expression vector pET-11a (Novagen, Madison WI). Purified RNase III had a specific activity of 1.9×10^5 units/mg (dimer) and was stored at −20 °C at a concentration of 0.1–0.5 mg/mL, in a buffer which contained 50% glycerol, 0.5 M KCl, 30 mM Tris-HCl (pH 8), 0.1 mM DTT, and 0.1 mM EDTA.

RNA Synthesis. RNAs were enzymatically synthesized *in vitro* according to the procedure of Milligan et al. (1987). A typical transcription reaction (25 μL) contained 1 mM of each rNTP, 20 μCi of [α-^{32}P]UTP, and 100 units of T7 RNA polymerase. RNAs were purified by electrophoresis in 15% polyacrylamide gels containing TBE buffer and 7 M urea and recovered from crushed gel bands by phenol extraction and ethanol precipitation. The internally ^{32}P-labeled RNAs had a specific activity of 2.8×10^4 dpm/pmol, as based on the specific activity of the input [^{32}P]UTP and the number of U residues in the transcripts. The preparation of nonradioactive RNA was carried out similarly, except that the RNAs were located in polyacrylamide gels using radioactive marker transcripts electrophoresed in separate lanes. Yields were determined by measuring the A_{260} and applying calculated extinction coefficients (Chelladurai et al., 1991). RNAs were 5′-^{32}P-end-labeled, either by enzymatic transcription in the presence of [γ-^{32}P]ATP or by treating dephosphorylated, nonradioactive RNA with T4 polynucleotide kinase and [γ-^{32}P]ATP. Mutations in several of the sequence variants were verified by base-specific enzymatic RNA sequencing reactions using 5′-end-labeled RNA (data not shown). The RNase III cleavage site of R1.1 RNA has been previously determined (Chelladurai et al., 1991).

In Vitro RNase III Processing Assays. Specific features of the processing assays are provided in the appropriate figure legends. "Physiological salt" reaction buffer[3] contains 250 mM potassium glutamate, 10 mM $MgCl_2$, 30 mM Tris-HCl (pH 7.5), 5 mM spermidine, 0.1 mM DTT, 0.1 mM EDTA, and 0.4 mg/mL *E. coli* tRNA. "Low-salt" reaction buffer was otherwise the same, except that it lacked potassium glutamate. RNase III was combined on ice with the ^{32}P-labeled RNA in Mg^{2+}-free reaction buffer, and the reaction was initiated by adding $MgCl_2$ to a final concentration of 10 mM (when necessary, RNase III was diluted on ice in Mg^{2+}-free buffer prior to its addition). Following incubation at the specified temperature, reactions were terminated by the addition of an equal volume of stop mix [20 mM EDTA, 89 mM Tris, 89 mM boric acid, 7 M urea, 20% sucrose (or 10 % glycerol), and 0.04% each of xylene cyanol and bromphenol blue]. Samples were electrophoresed (20–25 V/cm) in 15% polyacrylamide gels containing 7 M urea in TBE buffer. Autoradiography was performed at −70 °C, using Fuji RX film and intensifying screens. To quantitate the reactions, dried gels were analyzed by an Ambis radioanalytic imaging unit (2.8% counting efficiency).

Gel Electrophoretic Mobility Shift Assay. The gel mobility shift assay was performed as follows. To remove intermolecular RNA complexes, the ^{32}P-labeled RNAs were heated at 90 °C for 30 s in 10 mM Tris-HCl and 1 mM EDTA (pH 7.5). The RNA (5000 dpm, approximately 1 pmol) was then combined on ice with the indicated amount of RNase III in 10-μL reactions containing binding buffer [identical to physiological salt reaction buffer (see above), but lacking $MgCl_2$, and supplemented with 5 mM EDTA and 10% glycerol]. Following incubation at room temperature for 20 min, samples were placed on ice and then electrophoresed (10 V/cm) for 2.5–3 h at 5 °C in a 1.5 mm thick, linear (4–10%) polyacrylamide [0.1–0.26% bis(acrylamide)] gradient slab gels containing 0.5× TBE buffer. Separate lanes contained bromphenol blue and xylene cyanol markers. The gels were directly dried and exposed to Fuji RX film at −70 °C using intensifying screens. The amounts of free and bound RNAs were quantitated by radioanalytic imaging. The gel electrophoretic mobility and stability of the RNA–RNase III complex are relatively insensitive to the percent polyacrylamide and electrophoresis buffer used, as similar results were obtained using 8% polyacrylamide gels containing 1× TBE buffer (H.L. and A.W.N., unpublished observations).

RESULTS

The R1.1 GCAA Tetraloop Sequence Is Not Required for in Vitro Reactivity. The T7 R1.1 hairpin loop (Figure 1)

[3] Potassium glutamate enhances RNase III processing efficiency *in vitro* (Li et al., 1993), and it has been shown that glutamate is the predominant anionic species in the *E. coli* cytosol, at a concentration of approximately 250 mM (Leirmo et al., 1987).

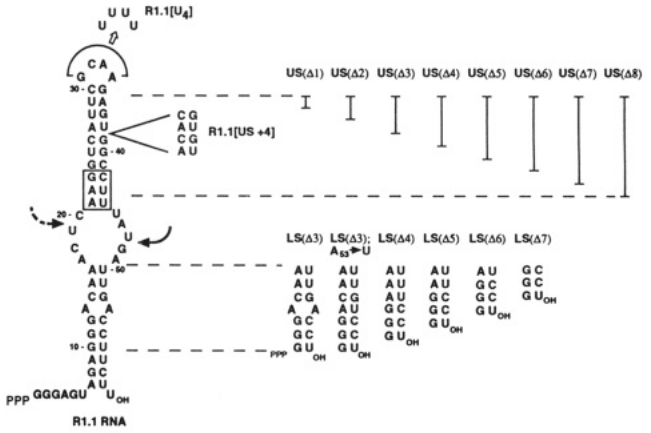

FIGURE 1: Primary and secondary structure of the T7 R1.1 processing signal and the sequences of specific R1.1 variants. The primary RNase III cleavage site (between U_{47} and G_{48}) is indicated by the solid arrow, and the secondary site (between U_{19} and C_{20}) is indicated by the dashed arrow. The boxed segment indicates the conserved sequence element (see text). In R1.1[U_4] RNA, the hairpin loop GCAA sequence is replaced by UUUU. R1.1[+4] RNA contains a 4 bp insertion in the upper stem at the indicated position. The missing base pairs in the upper stem (US) and lower stem (LS) deletion mutants are indicated by the vertical bars. The 5′ and 3′ ends of R1.1[LSΔ3] RNA correspond to nt positions 10 and 56, respectively, in R1.1 RNA.

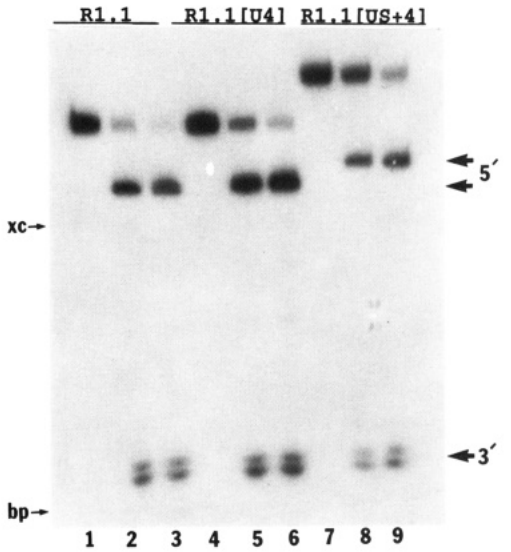

FIGURE 2: RNase III cleavage of the R1.1 upper stem sequence variants R1.1[U_4] and R1.1[US+4] RNA. Processing reactions (20 μL) were performed at 37 °C, and included 10 nM RNase III and 50 nM ^{32}P-labeled RNA in physiological salt reaction buffer (see Experimental Procedures). Aliquots (5 μL) were taken prior to (0 min), and at 2.5 and 40 min following initiation of the reaction, combined with an equal volume of stop mix, and analyzed by gel electrophoresis (see Experimental Procedures). Lanes 1–3, R1.1 RNA (0-, 2.5-, and 40-min reactions, respectively); lanes 4–6, R1.1[U_4] RNA (same order); lanes 7–9, R1.1[US+4] RNA (same order). The species marked 5′ carries the 5′ end of the RNA, while the 3′-end-containing cleavage product is indicated as 3′. The doublet nature of the small RNA product is due to the non-template-directed addition of an extra nucleotide to the 3′ terminus during RNA synthesis (Milligan et al., 1987). "xc" and "bp" refer to the positions of the xylene cyanol and bromphenol blue dye markers, respectively.

contains the GCAA sequence, which is also present in the T7 R0.3 processing signal (Dunn & Studier, 1983). The R1.1 tetraloop belongs to the GNRA sequence motif, which has been shown to stabilize RNA hairpins (Tuerck et al., 1988). To determine whether the GCAA tetraloop sequence is important for R1.1 RNA processing reactivity, an R1.1 variant was prepared which carries a UUUU tetraloop (R1.1[U_4] RNA; Figure 1). The reactivity of R1.1[U_4] RNA was measured in physiological salt buffer and compared to that of wild-type R1.1 RNA. The results, shown in Figure 2, reveal that R1.1[U_4] RNA undergoes cleavage with the same specificity and efficiency as the wild-type substrate (Figure 2, compare lanes 4–6 with lanes 1–3). We conclude that the GCAA tetraloop sequence is not important for *in vitro* reactivity of the R1.1 processing signal. However, this sequence element may be important for proper formation of the R1.1 processing signal during its synthesis *in vivo*.

R1.1 Processing Signal Variants with Shortened dsRNA Elements Are Accurately Processed but with Reduced Efficiencies. The molecular ruler model, as strictly interpreted, proposes that the scissile bond is determined by its distance from one end of the dsRNA element in an RNase III processing signal. To test this hypothesis, an R1.1 RNA variant was prepared which contained a 4 bp insertion in the upper stem (R1.1[US+4] RNA; Figure 1). If RNase III "measures" the R1.1 upper stem, then a 4 bp insertion could cause a corresponding 4 bp shift in the cleavage site. Alternatively, cleavage of additional phosphodiester bonds may occur if the lengthened dsRNA element provides additional enzyme binding sites. Figure 2 displays the *in vitro* cleavage reactivities of ^{32}P-labeled R1.1[US+4] RNA and wild-type R1.1 RNA. It is seen that R1.1[US+4] RNA is cleaved at a single site, with a reaction efficiency comparable to that of the R1.1 RNA (Figure 2, compare lanes 1–3 with lanes 7–9). The R1.1[US+4] RNA cleavage site corresponds to the canonical site, since the short (3′-end-containing) cleavage product exhibits the same gel electrophoretic mobility as the 13 nt R1.1 RNA cleavage product. The 5′-end-containing cleavage product of R1.1[US+4] RNA has a slower electrophoretic mobility than the corresponding R1.1 RNA species (Figure 2, compare lanes 2 and 3 with lanes 8 and 9), which reflects the additional 8 nt in the upper dsRNA stem. We conclude that lengthening the R1.1 upper stem by 4 bp does not alter scissile bond selection or processing signal reactivity (see Discussion).

Does decreasing the size of the R1.1 upper dsRNA stem influence cleavage site selection? A series of R1.1 deletion mutants were prepared, which exhibit progressively shortened upper stems (Figure 1). Low substrate concentrations were used, so that the processing reactivities would reflect changes in either K_m or k_{cat}. Cleavage reactivities were measured in low-salt as well as physiological salt reaction buffer, since it was previously shown that low salt promotes cleavage of otherwise unreactive substrates (Dunn, 1976; Gross & Dunn, 1987). The cleavage patterns obtained in physiological salt buffer of several of the deletion mutants are displayed in Figure 3, and the cleavage reactivities of all the mutants in both reaction buffers are summarized in Table I. The data show that shortening the R1.1 upper stem does not cause a corresponding shift in RNase III cleavage site. Specifically, for those deletion mutants which are reactive, the 3′-end-containing cleavage products comigrate with the corresponding wild-type substrate cleavage product (Figure 3). Note that the larger cleavage products (containing the transcript 5′ end and upper stem), exhibit progressively greater electrophoretic mobilities, reflecting the loss of bp in the upper stem. In contrast to its lack of involvement in processing selectivity, the R1.1 upper stem length markedly influences cleavage reactivity. The experiment in Figure 3 reveals a progressively diminished cleavage reactivity as the upper stem is shortened, and the deletion mutants which lack 5 bp or more are essentially

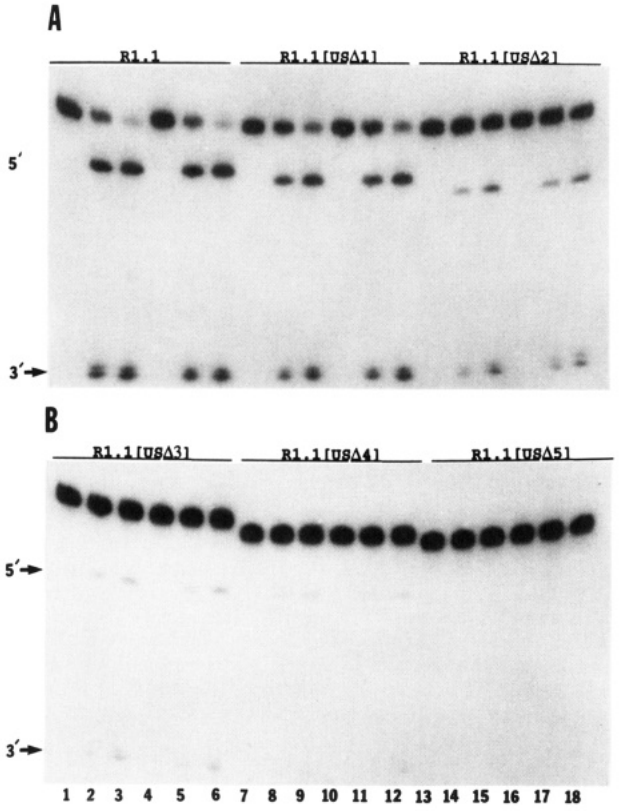

FIGURE 3: RNase III cleavage of R1.1 upper stem deletion mutants. The deletion mutants examined in this experiment are R1.1[USΔ1], R1.1[USΔ2], R1.1[USΔ3], R1.1[USΔ4], and R1.1[USΔ5] (Figure 1). Processing reactions (20 μL) included internally ^{32}P-labeled RNA (50 nM) and RNase III (10 nM) and were performed in duplicate at 37 °C in physiological salt reaction buffer (see Experimental Procedures). Following initiation of reaction, 5-μL aliquots were taken at 0, 2.5, and 40 min and analyzed by gel electrophoresis and radioanalytic imaging. The relative cleavage reactivities are summarized in Table I. (A) Cleavage of R1.1 RNA (lanes 1–3, 0, 2.5, 40 min; duplicate set in lanes 4–6); R1.1[USΔ1] RNA (lanes 7–9, 10–12, same order), and R1.1[USΔ2] RNA (lanes 13–15, 16–18, same order). (B) Cleavage of R1.1[USΔ3] RNA (lanes 1–3, 4–6), R1.1[USΔ4] RNA (lanes 7–9, 10–12), and R1.1[USΔ5] RNA (lanes 13–15, 16–18). The cleavage products which contain the transcript 5′ and 3′ ends are indicated by 5′ and 3′, respectively. Note the invariant size of the 3′-end-containing cleavage product, indicating recognition of the canonical cleavage site, and the progressively increased mobility of the larger cleavage product (containing the R1.1 upper stem), which carries the deletion.

unreactive in physiological salt buffer (Figure 3; Table I). However, low-salt buffer supports the cleavage of otherwise unreactive deletion mutants, such that only the 8 bp deletion mutant (R1.1[USΔ8] RNA) is unreactive (Table I). It is presently not known whether residual upper stem dsRNA structure persists in R1.1[USΔ8] RNA.

Cleavage site selection may alternatively (or in addition) involve the R1.1 lower dsRNA stem. This possibility was evaluated by measuring the processing reactivities (as described above) of R1.1 RNA variants exhibiting progressively shortened lower stems (Figure 1). Figure 4 displays the results of a representative analysis of the cleavage of R1.1[LSΔ5], R1.1[LSΔ6], and R1.1[LSΔ7] RNAs in low-salt reaction buffer. Table I summarizes the cleavage reactivities in both reaction buffers of all the deletion mutants. If the canonical cleavage site were utilized in all instances, then deletions within the lower dsRNA stem would result in a proportionately shortened 3′-end-containing cleavage product, without affecting the size (28 nt) of the upper-stem-containing RNA (the product of low-salt-promoted cleavage of the secondary as well as primary site). In fact, the R1.1 lower stem can be shortened without altering cleavage site selection, as the gel electrophoretic analysis reveals a progressively greater mobility of the 3′-end-containing cleavage product, with no change in the mobility of the 28 nt upper stem hairpin (Figure 4). However, the length of the lower stem influences reactivity, as enzymatic cleavage is progressively inhibited as the lower stem is shortened (Table I). With R1.1[LSΔ7] RNA (possessing a 3 bp lower stem), a small amount of accurate cleavage in physiological salt buffer is observed only at long reaction times and with longer autoradiographic exposures. Table I shows that several of the unreactive lower stem deletion mutants are processed in low-salt buffer. In particular, R1.1[LSΔ7] RNA undergoes a significant amount of accurate cleavage (Figure 4, lanes 17 and 18). R1.1 RNA variants with larger deletions in the lower stem have not been tested.

Comparison of the relative inhibitory effects of deletions within the R1.1 upper and lower stem suggests that the two dsRNA elements may play unequal (but nonetheless functionally complementary) roles in establishing R1.1 processing reactivity. Thus, RNase III cleavage of R1.1 RNA appears to exhibit a greater tolerance for deletions in the lower stem than in the upper stem (Table I). In addition, R1.1 secondary site cleavage (the product of which is just visible in Figure 3A, lanes 2,3 and 5,6) is suppressed by the introduction of even a single bp deletion in the upper stem but is not selectively inhibited (relative to the canonical site) by deletions in the lower stem (see Figure 4). The cleavage reactivities of R1.1 sequence variants which exhibit simultaneous deletions in the upper and lower stems have not yet been measured.

Effect of R1.1 Upper Stem Point Mutations on Processing Reactivity. It was previously shown that base pair substitutions within a conserved sequence motif (CUU/GAA) in the upper stem do not significantly inhibit or otherwise alter accurate *in vitro* enzymatic cleavage of R1.1 RNA (Chelladurai et al., 1991). Studies on other RNase III processing signals have shown that mutations which disrupt WC base-pairing within the conserved element can block cleavage *in vivo* (Saito & Richardson, 1981; Montanez et al., 1986; Altuvia et al., 1987). To assess the importance of WC base-pairing within the CUU/GAA element, several R1.1 variants were prepared which carried point mutations expected to disrupt WC base-pairing within this sequence. Two of the variants (R1.1[G_{24}→A] and R1.1[G_{23}→A] RNA) exhibit a G to A transition, each changing a separate GC bp to an AC bp (Figure 5A). R1.1[G_{24}→A] RNA formally corresponds to the HS9 mutation of the T7 R1.3 processing signal (Saito & Richardson, 1981), while R1.1[G_{23}→A] RNA carries a mutation corresponding to the *sib*2 lesion in the lambda P_L transcript RNase III processing signal (Montanez et al., 1986) and the r1 mutation in the lambda cIII mRNA RNase III processing signal (Altuvia et al., 1987). R1.1[$G_{23}G_{24}$→AA] RNA incorporates both mutations (Figure 5A). The two other R1.1 sequence variants (R1.1[$C_{41}C_{42}$→GG] and R1.1[$U_{43}U_{44}$→AA] RNA; Figure 5A) carry double point mutations, designed to more severely perturb the regular double-helical structure within the conserved element.

The cleavage reactivities of the R1.1 upper stem point mutants were assayed in physiological salt and low-salt reaction buffer, and the results are displayed in Figure 5B,C. When cleavage was observed, the canonical site was used, as indicated by the comigration of the 3′-end-containing cleavage products (not shown in Figure 5B,C). R1.1[G_{23}→A] RNA undergoes partial cleavage in physiological salt, compared to the wild-type substrate (Figure 5B, compare lanes 7–9 with lanes 1–3). However, R1.1[G_{23}→A] RNA cleavage efficiency is increased

Table I: Summary of Cleavage Reactivities of R.1 Processing Signal Variants Exhibiting Base Pair Deletions in the Upper or Lower dsRNA Stem

RNA[a]	R1.1	USΔ1	USΔ2	USΔ3	USΔ4	USΔ5	USΔ6	USΔ7	USΔ8
reactivity (+K)[b]	+++	+++	++	+	+	(–)	–	–	–
(–K)	+++	+++	+++	+++	+++	+++	++	(–)	–
RNA	R1.1	LSΔ3	LSΔ3′[c]	LSΔ4	LSΔ5	LSΔ6	LSΔ7		
reactivity (+K)	+++	+++	+++	++	++	+	(–)		
(–K)	+++	+++	+++	+++	+++	++	+		

[a] Refer to Figure 1 for the structures of the upper and lower stem deletion mutants. [b] *In vitro* processing reactions were performed in duplicate at 37 °C using internally ^{32}P-labeled substrate, as described under Experimental Procedures. Aliquots were withdrawn at 2.5 and 40 min following initiation of the reaction and analyzed by electrophoresis and radioanalytic imaging. "+K" indicates the use of physiological salt reaction buffer, and "–K" indicates the use of low-salt reaction buffer (see Experimental Procedures). [c] LSΔ3′ is R1.1[LSΔ3; A_{53}→U] (see Figure 1). The cleavage reactivities of the R1.1 variants are reported as follows: +++ indicates 50–100% conversion to product in 2.5 min; ++ indicates 10–50% conversion; + indicates 2–10% conservion. – indicates no detectable cleavage, either using radioanalytic imaging or upon extended autoradiographic exposure; (–) indicates that a minor amount of cleavage (<2% conversion to product) was observable in the autoradiogram but was below the limits of quantitation by radioanalytic imaging (the detectability limit was determined by the machine background of 0.6–0.8 cpm, which represents approximately 1% of the ^{32}P radioactivity loaded in each gel lane).

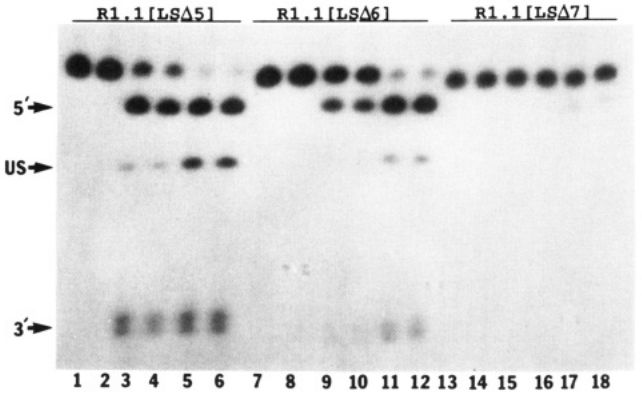

FIGURE 4: RNase III processing of R1.1 lower stem sequence variants. The experiment displayed shows the cleavage reactivities of internally ^{32}P-labeled R1.1[LSΔ5], R1.1[LSΔ6], and R1.1[LSΔ7] RNA (see Figure 1), measured in low-salt reaction buffer. Assays (20 μL) were performed in duplicate at 37 °C, using 50 nM RNA and 10 nM RNase III. Aliquots (5 μL) were removed at 0, 2.5, and 40 min following initiation of the reactions, added to an equal volume of stop mix, and analyzed by gel electrophoresis and radioanalytic imaging (see Experimental Procedures). The relative cleavage reactivities are summarized in Table I. Lanes 1, 3, 5 and 2, 4, 6, R1.1[LSΔ5] RNA (0, 2.5, and 40 min for each set); lanes 7, 9, 11, and 8, 10, 12, R1.1[LSΔ6] RNA (same order); lanes 13, 15, 17, and 14, 16, 18, R1.1[LSΔ7] RNA (same order). The 28 nt upper stem RNA hairpin (US), resulting from primary and secondary site cleavage (see Figure 1), is indicated. The cleavage products containing the transcript 5′ and 3′ ends are noted by 5′ and 3′, respectively.

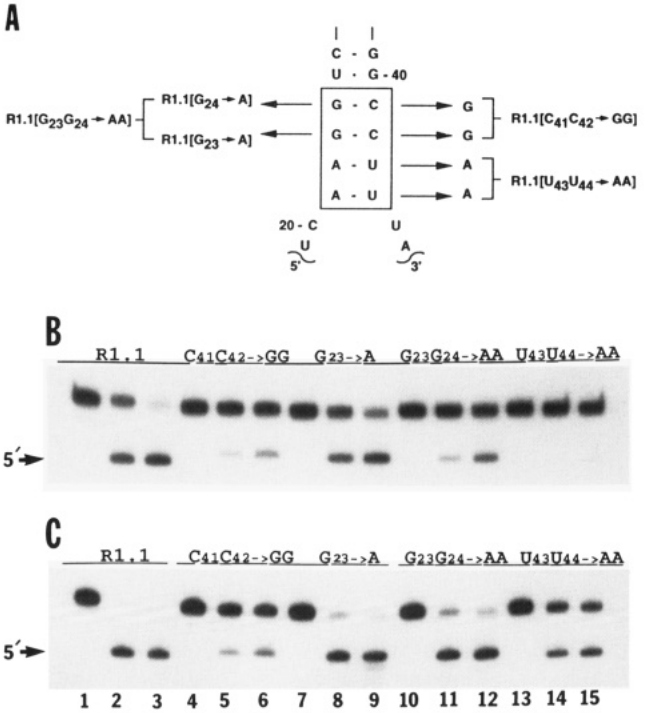

FIGURE 5: RNase III processing of R1.1 variants containing mutations in the conserved sequence element. (A) Diagram of the portion of the R1.1 upper stem, containing the CUU/GAA bp sequence (refer to Figure 1) and which shows the nucleotide changes. (B) *In vitro* processing reactivities of the R1.1 variants in physiological salt. (C) The same as in (A), except in low-salt reaction buffer. Processing reactions (20 μL) were performed using internally ^{32}P-labeled RNA at 37 °C in the indicated reaction buffer, as described under Experimental Procedures. Aliquots (5 μL) were removed at 0, 2.5, and 40 min following initiation of the reaction and analyzed by gel electrophoresis (see Experimental Procedures). Displayed are portions of the autoradiograms which show the precursor and the large (5′-end-containing) cleavage product. Lanes 1–3, R1.1 RNA (0, 2.5, 40 min); lanes 4–6, R1.1[$C_{41}C_{42}$→GG] (same order); lanes 7–9, R1.1[G_{23}→A] RNA (same order); lanes 10–12, R1.1-[$G_{23}G_{24}$→AA] RNA (same order); lanes 13–15, R1.1[$U_{43}U_{44}$→AA] RNA (same order). Only the cleavage product containing the transcript 5′ end is shown (denoted by 5′). The R1.1[G_{24}→A] RNA experiment is not shown, as the mutation in this variant caused early termination of transcription. The small amount of full-length RNA obtained, however, exhibited a reactivity comparable to that of R1.1[G_{23}→A] RNA and R1.1[$G_{23}G_{24}$→AA] RNA (B.S.C. and A.W.N., unpublished observations).

in low salt (Figure 5C, lanes 7–9). R1.1[G_{24}→A] RNA exhibits essentially the same cleavage reactivity as R1.1-[G_{23}→A] RNA, under both conditions (data not shown; see legend to Figure 5). The corresponding double point mutant (R1.1[$G_{23}G_{24}$→AA] RNA) also undergoes accurate cleavage in physiological salt buffer (Figure 5B, lanes 10–12), and the reaction occurs with greater efficiency in low-salt buffer (Figure 5C, lanes 10–12).

Interestingly, the use of low-salt reaction buffer does not increase the cleavage reactivity of R1.1[$C_{41}C_{42}$→GG] (compare Figure 5B,C, lanes 4–6). The partial cleavage reactivity may reflect an unreactive conformer subpopulation of R1.1[$C_{41}C_{42}$→GG] RNA. Alternatively, a mutation-imposed inhibition of substrate turnover may be significant.[4] The slightly slower electrophoretic mobility of the large cleavage product of R1.1[$C_{41}C_{42}$→GG] RNA (Figure 5B) probably reflects the partial denaturation of the mutant R1.1 upper stem during electrophoresis in the presence of 7 M urea. R1.1[$U_{43}U_{44}$→AA] RNA is resistant to cleavage in physiological salt (Figure 5B, lanes 13–15); however, its reactivity is greatly increased in low salt (Figure 5C, lanes 13–15).

[4] There is approximately a 5-fold molar excess of substrate over enzyme in these experiments. Partial cleavage is not due to loss of enzyme activity, since RNase III is stable for several hours under these reaction conditions (Li et al., 1993).

Perhaps the inhibitory effect reflects weakened enzyme binding, due to a formal enlargement of the R1.1 internal loop, which is partially compensated by lowering the salt concentration (see also below). In summary, these results show that accurate cleavage *in vitro* of the R1.1 processing signal exhibits a significant degree of tolerance toward disruption of WC base-pairing within the conserved CUU/GAA element. Neither the HS9 nor the *sib2*/r1 mutation strongly inhibits accurate *in vitro* enzymatic cleavage of the R1.1 processing signal, and the data support the previous conclusion (Chelladurai et al., 1991) that the CUU/GAA element alone does not dictate *in vitro* RNase III processing selectivity or reactivity (see also Discussion).

The R1.1 Processing Signal Internal Loop Enforces Single Enzymatic Cleavage. A number of RNase III processing signals feature an internal loop, which varies in sequence and size.[5] Single enzymatic cleavage is usually observed when the scissile bond is within the internal loop (Robertson, 1982; Dunn, 1982). However, it is not clear whether the internal loop structure *per se* is required for processing reactivity. To examine this, two R1.1 variants were prepared in which the internal loop is WC base-paired. In R1.1[WC-L] RNA (61 nt), the internal loop left-side sequence is fully complementary to the right-side sequence, while in R1.1[WC-R] RNA (59 nt) the right-side sequence is complementary to the left-hand sequence (Figure 6A). The greater gel electrophoretic mobilities of R1.1[WC-L] RNA and R1.1[WC-R] RNA, compared to that of R1.1 RNA (Figure 6B, compare lanes 6 and 10 with lane 2), presumably reflect the maintenance of the compact hairpin structure during gel electrophoresis in the presence of 7 M urea. Also, preliminary enzymatic structure-probing experiments (H.L. and A.W.N., unpublished experiments) indicate that R1.1[WC-L] RNA is fully base-paired in this region.

The RNase III processing reactivities of ^{32}P-labeled R1.1[WC-L] and R1.1[WC-R] RNA were determined. The results (Figure 6B) demonstrate that the R1.1 internal loop is not needed for enzymatic reactivity. Efficient cleavage of R1.1[WC-L] RNA and R1.1[WC-R] RNA occurs at two sites, yielding three discrete products (Figure 6B, lanes 7 and 11). The canonical scissile bond is cleaved in R1.1[WC-L] RNA, as indicated by the comigration of the smaller 3′-end-containing fragment with the corresponding R1.1 RNA cleavage product (Figure 6B, compare lanes 7 and 3). Cleavage of R1.1[WC-R] RNA generates a species which is one nucleotide shorter than the R1.1[WC-L] RNA and R1.1 RNA cleavage products (Figure 6B, compare lane 11 with lanes 7 and 3), which is the expected result if the canonical site is used (see Figure 6A). The additional cleavage site in R1.1[WC-L] RNA and R1.1[WC-R] RNA occurs in the RNA strand opposite the canonical site and is offset by two nt (between U_{20} and A_{21} in R1.1[WC-L] RNA and between U_{19} and C_{20} in R1.1[WC-R] RNA; Figure 6A). The position of the second site is inferred from the production of (i) the 28 nt upper stem hairpin, which is the same size in R1.1-[WC-L] and R1.1[WC-R] RNA (Figure 6B, lanes 7 and 11), and (ii) the 5′-end-containing cleavage product, which is predicted to be one nucleotide shorter in R1.1[WC-R] RNA than in R1.1[WC-L] RNA (Figure 6B, lanes 7 and 11). In support of this, RNase III cleavage of 5′-^{32}P-labeled R1.1-[WC-L] RNA or R1.1[WC-R] RNA yields the 5′ fragment as the only radiolabeled product (Figure 6B, lanes 9 and 13), demonstrating that this RNA carries the R1.1 RNA 5′ end. Finally, the location of the second cleavage site in R1.1-[WC-L] RNA and R1.1[WC-R] RNA corresponds to the R1.1 RNA secondary site (between U_{19} and C_{20}; Figure 1) whose cleavage reactivity increases in low-salt buffer (Chelladurai et al., 1991; see also Figure 4).

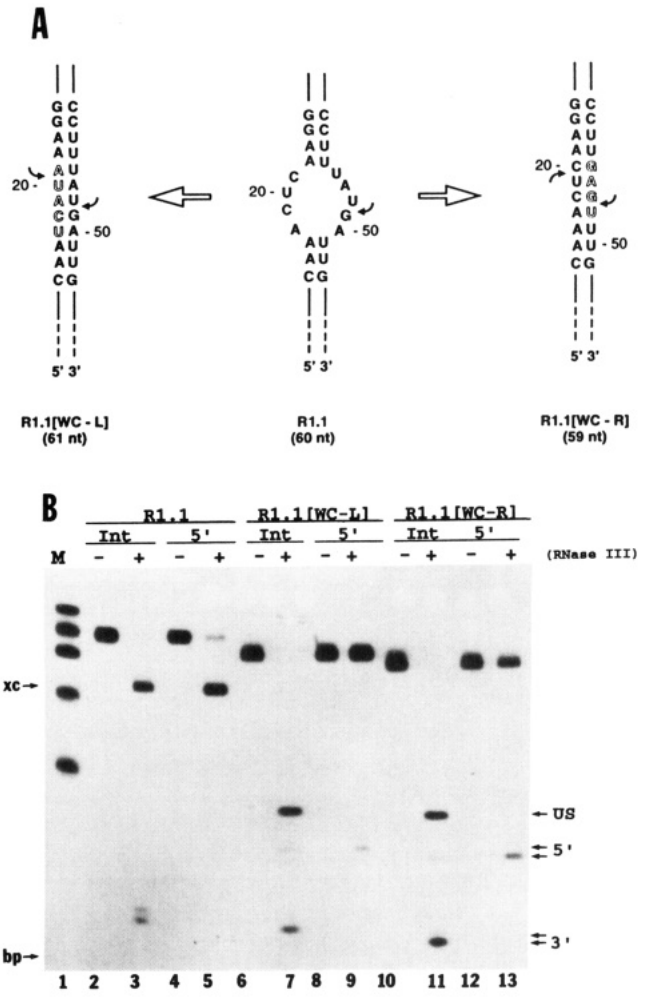

FIGURE 6: RNase III reactivity of R1.1 variants with a WC base-paired internal loop. (A) Diagram of the R1.1 processing signal internal loop, also showing the corresponding structures of R1.1[WC-L] RNA (61 nt) and R1.1[WC-R] RNA (59 nt). The RNase III cleavage sites are indicated by arrows. (B) Analysis of RNase III cleavage of internally ^{32}P-labeled or 5′-^{32}P-labeled R1.1[WC-L] and R1.1[WC-R] RNAs. 5′-End-labeling was carried out by including [γ-^{32}P]ATP (100 μCi) in the transcription reaction, as described under Experimental Procedures (the 5′ nucleotide is an A for these RNAs; see Figure 1). The RNAs were incubated with RNase III at 30 °C in reaction buffer in which the potassium glutamate component was replaced by 100 mM sodium chloride. Lanes 2 and 3, internally radiolabeled R1.1 RNA (600 dpm), without or with RNase III; lanes 4 and 5, 5′-end-labeled R1.1 RNA, without or with RNase III; lanes 6 and 7, internally radiolabeled R1.1[WC-L] RNA, without or with RNase III; lanes 8 and 9, 5′-end-labeled R1.1[WC-L] RNA (same order); lanes 10 and 11, internally radiolabeled R1.1[WC-R] RNA, without or with RNase III; lanes 12 and 13, 5′-end-labeled R1.1[WC-R] RNA (same order). "US" denotes the 28 nt R1.1 upper stem hairpin, resulting from double cleavage; "5′" denotes the 5′-end-containing fragment; and "3′" denotes the product carrying the R1.1 3′ end. Lane 1 displays RNA size markers. From top to bottom, the sizes are 73, 63, 55, 44, and 30 nt. "xc" and "bp" refer to the positions of the xylene cyanol and bromphenol blue dyes, respectively.

[5] The exact conformation of the R1.1 internal loop is presently unclear. However, enzymatic and chemical structure probing experiments indicate a helical (or quasi-helical) structure (H.L. and A.W.N., unpublished results), and proton NMR analysis of the R1.1 processing signal (D. Schweisguth, B.S.C., A.W.N., and P. B. Moore, in preparation) has identified slowly exchanging imino protons, several of which may be localized to the internal loop.

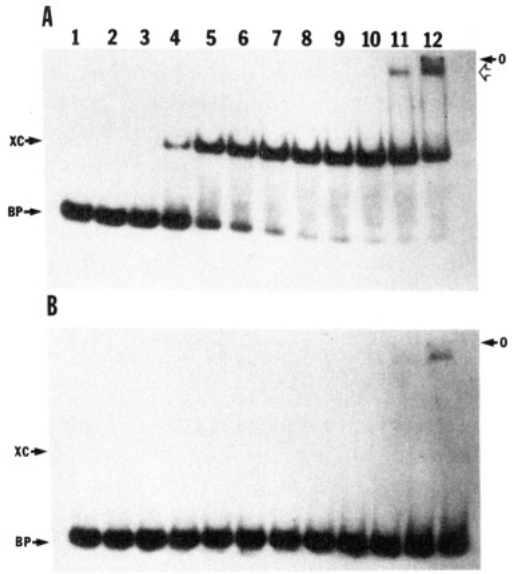

FIGURE 7: Gel mobility shift analysis of the R1.1 RNA–RNase III interaction. Internally ^{32}P-labeled RNA (5000 dpm; 1.5 pmol) was combined with RNase III in binding buffer and then subjected to nondenaturing gel electrophoresis (see Experimental Procedures). The gel was dried and subjected to autoradiography and radioanalytic imaging. The quantitative analysis of the R1.1[WC-L] RNA experiment (panel A) is presented in Figure 9. The R1.1 RNA experiment is presented in panel B. Lane 1, no RNase III; lane 2, 0.1 pmol of RNase III (dimer); lane 3, 0.5 pmol; lane 4, 1 pmol; lane 5, 2 pmol; lane 6, 3 pmol; lane 7, 5 pmol; lane 8, 7 pmol; lane 9, 10 pmol, lane 10, 20 pmol; lane 11, 40 pmol; lane 12, 60 pmol. On the right-hand side, "O" marks the origin of electrophoresis, and the open arrow (panel A) indicates the position of the *rnc* polypeptide, as revealed by Coomassie staining. On the left-hand side, "xc" and "bp" indicate the positions of the xylene cyanol and bromphenol blue dye markers, respectively.

Preliminary kinetic assays indicated a different reactivity of R1.1[WC-L] RNA and R1.1[WC-R] RNA, compared to that of R1.1 RNA. To determine the effects of a fully base-paired internal loop on processing reactivity, the steady-state kinetic parameters (K_m, k_{cat}) for R1.1[WC-L] RNA cleavage were measured, and compared to those of R1.1 RNA. The initial cleavage rates were measured in physiological salt reaction buffer as a function of substrate concentration. For R1.1[WC-L] RNA, production of the 28 nt upper stem was followed, while for R1.1 RNA, production of the 47 nt single cleavage product was followed. The K_m for R1.1[WC-L] RNA was 37 nM, while that for R1.1 RNA was 330 nM. The k_{cat} for R1.1[WC-L] RNA was 0.58 min^{-1}, while that for R1.1 RNA was 1.8 min^{-1} (37 °C). The approximately 9-fold lower K_m value for R1.1[WC-L] RNA, relative to that for R1.1 RNA, indicates that a fully base-paired internal loop confers a higher enzyme binding affinity (see also below). The approximately 3-fold lower k_{cat} indicates that a double-stranded internal loop retards a process occurring in the E–S complex, perhaps product release (see Discussion).

R1.1 RNA Undergoes a Gel Electrophoretic Mobility Shift with Added RNase III. Determination of RNase III binding to a processing signal, without concomitant cleavage, could permit a systematic correlation of binding affinity with processing signal structure and reactivity. To determine whether nondenaturing polyacrylamide gel electrophoresis could separate RNase III-bound from unbound processing substrate, ^{32}P-labeled R1.1 RNA was incubated with specific amounts of RNase III in (Mg^{2+}-free) binding buffer and then subjected to electrophoresis at 5 °C in a nondenaturing polyacrylamide gel. The results of the experiment are displayed in Figure 7B. An electrophoretically shifted RNA species is observed, but only at very high RNase III concentrations (Figure 7B, lanes 11 and 12). The shifted RNA species occurs near the origin of electrophoresis and overlaps the position of RNase III, as revealed by Coomassie staining (indicated by the open arrow in Figure 7A). The shifted R1.1 RNA probably reflects a nonspecific interaction of the RNA with a large excess of RNase III. A range of binding conditions and electrophoresis protocols were tested and provided essentially the same result. We conclude that R1.1 RNA–RNase III complex is unstable toward nondenaturing gel electrophoresis.

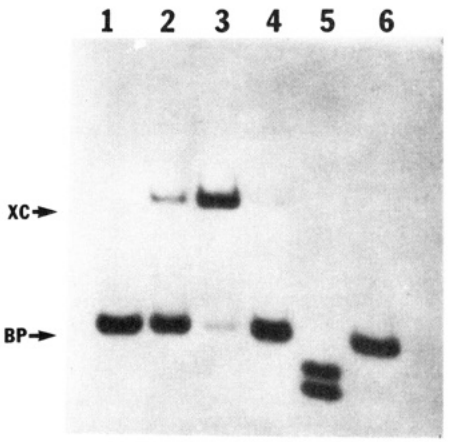

FIGURE 8: Specificity of the processing signal–RNase III interaction. Internally ^{32}P-labeled R1.1[WC-L] RNA (5000 dpm; 1.5 pmol) was combined with the indicated components in binding buffer and then subjected to electrophoresis in a nondenaturing polyacrylamide gel (see Experimental Procedures). Lane 1, no added RNase III; lane 2, 1 pmol of RNase III (dimer); lane 3, 5 pmol; lane 4, 5 pmol of RNase III plus 100 pmol of unlabeled R1.1[WC-L] RNA; lane 5, 5 pmol of RNase III, incubated in binding buffer containing 10 mM Mg^{2+}; lane 6, addition of 45 pmol of T7 RNA polymerase. "xc" and "bp" indicate the positions of the xylene cyanol and bromphenol blue dye markers, respectively.

The gel electrophoretic mobility of R1.1[WC-L] RNA in the presence of RNase III was also examined, as the smaller K_m and k_{cat} values indicated a greater binding affinity (see above). In contrast to R1.1 RNA, incubation of R1.1-[WC-L] RNA with relatively low amounts of RNase III produces an electrophoretically shifted species, migrating approximately halfway between free RNA and the origin (Figure 7A). The amount of the shifted RNA is protein-dependent, and essentially complete conversion of free to shifted RNA is obtained as the protein concentration is increased. The electrophoretic mobility shift of R1.1-[WC-L] RNA is dependent on temperature, as electrophoresis at room temperature did not yield this species (data not shown). The diffuse smear of ^{32}P radioactivity occurring between free and RNase III-shifted R1.1[WC-L] RNA (Figure 7A, lanes 4–12) probably represents dissociation of the protein–RNA complex during electrophoresis, since it is not observed in the absence of RNase III (Figure 7A, lane 1) and since only the diffuse smear was obtained when electrophoresis was performed at room temperature (data not shown). Similar to the results obtained with R1.1 RNA, a shifted R1.1[WC-L] RNA species also occurs near the origin at high protein concentrations (Figure 7B, lane 12). This species probably represents a nonspecific association of R1.1[WC-L] RNA with RNase III.

To determine the specificity of the RNase III-dependent R1.1[WC-L] RNA mobility shift, additional experiments were performed, the results of which are presented in Figure 8. In agreement with the first experiment, the data show that the

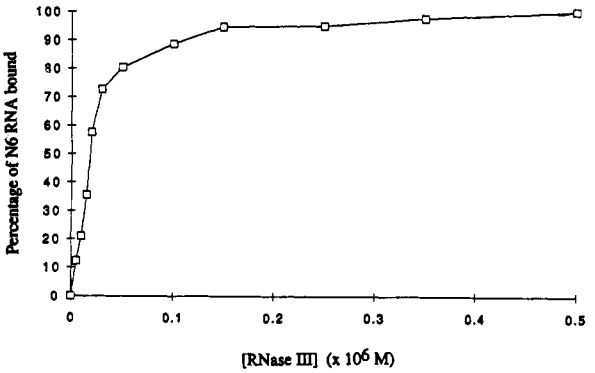

FIGURE 9: Quantitative analysis of R1.1[WC-L] RNA binding to RNase III. Since these experiments necessitated the use of low concentrations of RNA, R1.1[WC-L] RNA was 5′-^{32}P-end-labeled to a high specific activity. Specifically, ^{32}P-labeled substrate was prepared by dephosphorylating unlabeled R1.1[WC-L] RNA with calf intestinal phosphatase, followed by treatment with T4 polynucleotide kinase and [γ-^{32}P]ATP. The ^{32}P-labeled RNA was purified by gel electrophoresis. Gel mobility shift assays were performed as described under Experimental Procedures, using approximately 3 fmol (20 000 dpm) of RNA and the same range of RNase III concentrations as reported in the legend to Figure 7. The K_d value was determined by double-reciprocal analysis of the results of three independent experiments.

mobility shift of ^{32}P-labeled R1.1[WC-L] RNA is dependent on RNase III (Figure 8, compare lanes 2 and 3 with lane 1). The inclusion of excess nonradioactive R1.1[WC-L] RNA in the binding reaction blocks the shift (presumably by direct competition) of the ^{32}P-labeled RNA (Figure 8, compare lane 4 with lane 2). The inhibition is RNA-specific, since excess tRNA (present in all assays) had no effect and since substituting a ^{32}P-labeled, nonspecific plasmid run-off transcript did not yield a gel-shifted species (data not shown). Addition of Mg^{2+} to the binding reaction, at a concentration sufficient to support enzymatic cleavage, resulted in production of two RNA species, both of which electrophorese more rapidly than the unbound RNA (Figure 8, lane 5). Thus, the RNase III-shifted R1.1[WC-L] RNA in Mg^{2+}-free buffer is not a cleavage product possessing an anomalous electrophoretic mobility, nor is it a cleavage product complexed with RNase III. Finally, the substitution of RNase III by an equivalent amount of purified T7 RNA polymerase does not alter R1.1[WC-L] RNA electrophoretic mobility (Figure 8, lane 6). Taken together, these experiments show that RNase III can bind a fully base-paired R1.1 sequence variant in Mg^{2+}-free buffers to yield a complex which can be isolated by gel electrophoresis. In contrast, the R1.1 internal loop apparently destabilizes the protein–RNA complex to the extent that it is unstable toward gel electrophoresis.

A quantitative analysis of the data in Figure 7B can provide an estimate of the K_d of the RNase III–R1.1[WC-L] RNA complex. The partial dissociation of enzyme-bound RNA was taken into account in the calculations. Thus, the amount of unbound RNA was measured, allowing calculation of the fraction of RNA engaged in the complex, which was then plotted as a function of the amount of added RNase III (Figure 9). The data indicate that the K_d (5–6 °C) for the R1.1[WC-L] RNA–RNase III complex is 35 nM (the average of three independent determinations). The K_d value can be compared to the K_m of 37 nM for R1.1[WC-L] RNA cleavage (see above).

DISCUSSION

This study has shown that enzymatic selection of the cleavage site in an RNase III processing signal does not involve measurement from one end of the resident dsRNA element. Thus, the lengths of the upper or lower dsRNA stems in the phage T7 R1.1 processing signal do not specify the scissile bond. These results can be contrasted with those from studies on the yeast tRNA splicing endonuclease, in which it was shown that the length of the anticodon stem determines the intron 5′ and 3′ cleavage sites (Reyes & Abelson, 1988). The comparable processing efficiencies of R1.1[US+4] RNA and R1.1[WT] RNA suggest that optimal cleavage reactivity may be realized with the overall size of the R1.1 RNA, which is a little larger than two full turns of the A-form double helix (assuming that the internal loop contributes the equivalent of 4 bp). However, the length of the dsRNA element can influence processing efficiency, as R1.1 RNA cleavage reactivity is progressively reduced as either the upper or lower dsRNA stem is shortened. Perhaps the deletion of base pairs causes a conformational change at or near the scissile bond, thereby inhibiting cleavage. Alternatively, base pair deletions may destroy enzyme–RNA contacts, reducing substrate binding affinity. Preliminary kinetic studies of the R1.1 deletion mutants support the latter possibility (B.S.C., H..L., and A.W.N., unpublished experiments). Moreover, hydroxyl radical footprinting and ethylation interference experiments indicate that RNase III touches R1.1 RNA at specific sites in the upper and lower dsRNA stems, at some distance from the scissile bond (H.L. and A.W.N., unpublished experiments). The cleavage in low-salt buffer of otherwise unreactive R1.1 deletion mutants may reflect enhanced binding of RNase III to the smaller, suboptimal substrates. The involvement of both upper and lower dsRNA stems in processing reactivity is not surprising, as the twofold symmetry of the double helix and the homodimeric nature of RNase III implies a symmetrical interaction between enzyme and substrate (Court, 1993). This type of interaction is also suggested by the preliminary footprinting and interference assays.

The hierarchical processing reactivities of the R1.1 upper and lower stem deletion mutants may be useful in assessing the cleavage efficiencies of other RNase III processing signals. For example, substrates which formally possess a shorter dsRNA element may be inefficiently cleaved *in vivo*. If RNase III processing triggers a subsequent reaction (e.g., mRNA turnover or enhanced translation), partial cleavage reactivity may confer regulatory control, especially if RNAse III processing *in vivo* may be influenced by the salt concentration (Dunn, 1976; Saito & Richardson, 1981) or through covalent activation of the enzyme (Mayer & Schweiger, 1983). The autoregulation of RNase III expression (Bardwell et al., 1989) may in part rely on a relatively reduced cleavage reactivity of the *rnc* operon RNase III processing signal (containing an approximately 15 bp dsRNA element). Experiments currently underway are attempting to measure and correlate the *in vivo* reactivities of R1.1 variants which exhibit a broad range of *in vitro* cleavage efficiencies.

The R1.1 internal loop does not establish reactivity *per se* but instead enforces single cleavage under physiological conditions. Altering the internal loop to a fully base-paired structure allows coordinate double cleavage, which is the observed reactivity pattern for regular dsRNA substrates. The K_m for R1.1[WC-L] RNA cleavage, compared to that for the wild-type substrate, indicates that the internal loop decreases enzyme binding affinity by approximately 9-fold. Moreover, R1.1[WC-L] RNA (but not R1.1 RNA) can form a complex with RNase III which is stable toward electrophoresis in nondenaturing polyacrylamide gels. Preliminary experiments have shown that the R1.1[WC-L] RNA–RNase

III complex can also be retained on nitrocellulose filters (K.Z. and A.W.N., unpublished results). However, the filter-bound complex is somewhat labile, which is consistent with the partial dissociation of the enzyme–substrate complex during electrophoresis in nondenaturing gels (see Results). Since the K_m value for R1.1[WC-L] processing is comparable to the K_d value of the R1.1[WC-L] RNA–RNase III complex, it is likely that tighter substrate binding reflects a slower rate of substrate dissociation. The approximately 3-fold lower k_{cat} for R1.1[WC-L] RNA cleavage, compared to that of R1.1 RNA, suggests that the reduced substrate dissociation may also be reflected in a slower product release step. The gel mobility shift assay will be useful in determining the relative binding affinities of RNase III processing signal mutants, as well as in structure-probing studies on the enzyme–substrate complex.

How might the internal loop structure establish single cleavage? Perhaps cutting at the canonical site is immediately followed by a local RNA conformational change—which is not available to a dsRNA substrate—thereby enhancing enzyme dissociation and aborting the second cleavage step. The activation of R1.1 secondary site processing in low salt may be due to inhibition of substrate dissociation following initial cleavage, thereby enhancing the efficiency of the second chemical step. This model also suggests that the double cleavage of a dsRNA substrate is not necessarily concerted but is instead a stepwise process in which the two steps can be uncoupled. Preliminary experiments indicate that R1.1-[WC-L] RNA processing occurs through random order initial cutting (K.Z., B.S.C., and A.W.N., unpublished experiments). However, it is interesting to note that the structural perturbation introduced by the R1.1 internal loop directs cleavage of only the 3′-end-proximal (canonical) site, while no RNase III processing signals have yet been identified which undergo single cleavage at a 5′-end-proximal (secondary) site.

What are the functional consequences of internal loop-directed single cleavage of a T7 mRNA primary site? The upstream RNA segment would carry the upper stem hairpin, which would provide a block to the degradative action of cellular 3′ → 5′ exoribonucleases (Gottesman et al., 1982; McLaren et al., 1991). The known chemical stability of processed T7 mRNAs (Dunn & Studier, 1983) is in part due to the 3′ terminal hairpins (Panayotatos & Truong, 1985). However, the internal loop weakens substrate binding. This would seem to confer a kinetic disadvantage to the T7 processing signals, compared to cellular dsRNA substrates (e.g., in the 30S rRNA precursor) which presumably possess higher enzyme affinities and which may be present in greater amounts. The presumptive disadvantage may be compensated by the T7-induced shutoff of host RNA synthesis (Brunovskis & Summers, 1971; McAllister & Barrett, 1977) and the T7 protein kinase-dependent phosphorylation of RNase III, which stimulates processing activity (Mayer & Schweiger, 1983).

The question remains as to the nature of RNase III processing signal recognition elements. Cleavage is strongly inhibited in a specific R1.1 double point mutant (R1.1-[$U_{43}U_{44}$→AA] RNA) which exhibits disruption of two AU bp in the conserved CUU/GAA element. This does not necessarily imply an essential involvement of the conserved sequence element, as this R1.1 variant formally exhibits an enlarged internal loop, which may be inhibitory (compare the difference in enzyme binding affinities of R1.1 RNA and R1.1[WC-L] RNA). Moreover, R1.1 sequence variants which carry bp substitutions in the conserved element are accurately processed *in vitro* (Chelladurai et al., 1991). Neither the HS9 mutation of the T7 R1.3 processing signal (Saito & Richardson, 1981) nor the *sib*2 mutation of the lambda P_L transcript RNase III processing signal (Montanez et al., 1986) strongly inhibits processing when present in the R1.1 RNA substrate. Perhaps these mutations are only effective in their original contexts, and may also reflect the possible degenerate nature of the RNase III identity elements (see below). However, it should be noted that the HS9 mutation blocks only secondary site cleavage of the R1.3 substrate (Saito & Richardson, 1981). Alternatively, RNase III processing *in vivo* may be considerably more sensitive to alterations in processing signal structure, which may be a consequence of possible limiting amounts of RNase III *in vivo*, competition between processing substrates, and additional factors not present in the *in vitro* system. The comparison of *in vivo* and *in vitro* processing reactivities of selected R1.1 point and deletion mutants should be informative in this regard. The systematic *in vitro* biochemical analysis of RNase III processing signal mutants may contain other problems of interpretation. For example, RNase III processing signals can have overlapping functions *in vivo* [e.g., see Montanez et al. (1986)], which could impose additional sequence and structural constraints. The application of *in vitro* genetic selection techniques (Tuerck & Gold, 1990; Ellington & Szostak, 1990)—bearing in mind the potential functional importance of a larger set of statistically significant, base-paired sequence elements in RNase III processing signals (Krinke & Wulff, 1990)—should allow identification of RNA sequences that are optimal ligands, unconstrained by additional functional demands.

The potential involvement of divalent metal ion in RNase III processing selectivity must also be addressed. Recent studies on specific restriction enzymes have shown that discrimination between cognate and noncognate cleavage sites can occur during the approach to the reaction transition state, through a divalent metal ion-mediated mechanism (Vermote & Halford, 1992; Thielking et al., 1992). It is therefore unclear whether the RNase III–R1.1 RNA complex which lacks Mg^{2+} accurately portrays an obligatory participant in the processing pathway. The involvement of divalent metal ion in recognition and discrimination may be assessed through protein footprinting, or *in vitro* genetic selection experiments, using divalent cations which cannot support cleavage, but may occupy the Mg^{2+} binding site(s) (e.g., Zn^{2+}; Li et al., 1993). Alternatively, a mutant RNase III may be employed which can bind substrate but cannot carry out Mg^{2+}-supported cleavage (Court, 1993). The identification of processing signal variants which bind RNase III but are resistant to cleavage may permit distinguishing between substrate discrimination that occurs in the binding step or catalytic step and further define the role of RNA sequence in RNase III recognition and catalysis.

ACKNOWLEDGMENT

We thank A. Rosenberg for providing the plasmid clone of the T7 RNA polymerase gene (pAR1219), June Snow of the Wayne State Macromolecular Core Facility for synthesis of DNA oligonucleotides, and Dr. Michael Hagen for instruction on the Ambis radioanalytic imaging unit.

REFERENCES

Altman, S., Guerrier-Takada, C., Frankfort, H. M., & Robertson, H. D. (1982) in *Nucleases* (Linn, S. J., & Roberts, R. J., Eds.) pp 243–274, Cold Spring Harbor Laboratory Press, Cold Spring Harbor, NY.

Altuvia, S., Locker-Giladi, H., Koby, S., Ben-Nun, O., & Oppenheim, A. B. (1987) *Proc. Natl. Acad. Sci. U.S.A. 84*, 6511–6515.
Bardwell, J. C. A., Regnier, P., Chen, S. M., Nakamura, Y., Grunberg-Manago, M., & Court, D. L. (1989) *EMBO J. 8*, 3401–3407.
Bram, R. J., Young, R. A., & Steitz, J. A. (1980) *Cell 19*, 393–401.
Brawerman, G., & Belasco, J. G. (1993) *Control of mRNA Decay*, Academic Press, New York.
Brunovskis, I., & Summers, W. C. (1971) *Virology 45*, 224–231.
Chelladurai, B. S., Li, H. L., & Nicholson, A. W. (1991) *Nucleic Acids Res. 19*, 1759–1766.
Court, D. (1993) in *Control of mRNA Decay* (Brawerman, G., & Belasco, J. G., Eds.), Academic Press, New York.
Daniels, D. L., Subbarao, M. N., Blattner, F. R. & Lozeron, H. A. (1988) *Virology 167*, 568–577.
Deutscher, M. (1988) *Trends Biochem. Sci. 13*, 136–139.
Deutscher, M. (1990) *Prog. Nucleic Acids Res. 39*, 209–240.
Dunn, J. J. (1976) *J. Biol. Chem. 251*, 3807–3814.
Dunn, J. J. (1982) in *The Enzymes* (Boyer, P., Ed.) Vol. 15, pp 485–499, Academic Press, New York.
Dunn, J. J., & Studier, F. W. (1983) *J. Mol. Biol. 166*, 477–535.
Ellington, A. D., & Szostak, J. W. (1990) *Nature 346*, 818–822.
Faubladier, M., Cam, K., & Bouche, J-P. (1990) *J. Mol. Biol. 212*, 461–471.
Gegenheimer, P., & Apirion, D. (1981) *Microbiol. Rev. 45*, 502–541.
Gottesman, M., Oppenheim, A. B., & Court, D. L. (1982) *Cell 29*, 727–728.
Grodberg, J., & Dunn, J. J. (1988) *J. Bacteriol. 170*, 1245–1253.
Gross, G., & Dunn, J. J. (1987) *Nucleic Acids Res. 15*, 431–442.
King, T. C., Sirdeskmukh, R., & Schlessinger, D. (1986) *Microbiol. Rev. 50*, 428–451.
Kramer, R. A., Rosenberg, M., & Steitz, J. A. (1977) *J. Mol. Biol. 89*, 767–776.
Krinke, L., & Wulff, D. L. (1990) *Nucleic Acids Res. 18*, 4809–4815.
Leirmo, S., Harrison, C., Cayley, D. S., Burgess, R. R., & Record, M. T. (1987) *Biochemistry 26*, 2095–2101.
Li, H-L., Chelladurai, B. S., Zhang, K., & Nicholson, A. W. (1993) *Nucleic Acids Res. 21*, 1919–1925.
Mayer, J. E., & Schweiger, M. (1983) *J. Biol. Chem. 258*, 5340–5343.
McAllister, W. T., & Barrett, C. L. (1977) *J. Virol. 23*, 543–553.
McLaren, R. S., Newbury, S. F., Dance, G. S. C., Causton, H. C., & Higgins, C. F. (1991) *J. Mol. Biol. 221*, 81–95.
Milligan, J. F., Groebe, D. F., Witherell, G. W., & Uhlenbeck, O. C. (1987) *Nucleic Acids Res. 15*, 8783–8798.
Montanez, C., Bueno, J., Schmeissner, U., Court, D. L., & Guarneros, G. (1986) *J. Mol. Biol. 191*, 29–37.
Nicholson, A. W. (1992) *Biochim. Biophys. Acta 1129*, 318–322.
Nicholson, A. W., Niebling, K. R., McOsker, P. L., & Robertson, H. D. (1988) *Nucleic Acids Res. 16*, 1577–1591.
Oakley, J. L., & Coleman, J. E. (1977) *Proc. Natl. Acad. Sci U.S.A. 74*, 4266–4270.
Panayotatos, N., & Truong, K. (1985) *Nucleic Acids Res. 13*, 2227–2240.
Pragai, B., & Apirion, D. (1981) *J. Mol. Biol. 153*, 619–630.
Regnier, P., & Grunberg-Manago, M. (1990) *Biochimie 72*, 825–834.
Reyes, V. M., & Abelson, J. (1988) *Cell 55*, 719–730.
Robertson, H. D. (1977) in *Nucleic Acid-Protein Recognition* (Vogel, H., Ed.) pp 549–568, Academic Press, New York.
Robertson, H. D. (1982) *Cell 30*, 669–672.
Rosenberg, M., Kramer, R. A., & Steitz, J. A. (1977) *J. Mol. Biol. 89*, 777–782.
Saito, H., & Richardson, C. C. (1981) *Cell 27*, 533–542.
Steege, D. A., Cone, K. C., Queen, C., & Rosenberg, M. (1987) *J. Biol. Chem. 262*, 17651–17658.
Thielking, V., Selent, U., Kohler, E., Landgraf, A., Wolfes, H., Alves, J., & Pingoud, A. (1992) *Biochemistry 31*, 3727–3732.
Tuerck, C., & Gold, L. (1990) *Science 249*, 505–510.
Tuerck, C., Gauss, P., Thermes, C., Groebe, D. R., Gayle, M., Guild, N., Stormo, G., D'Aubenton-Carafa, Y., Uhlenbeck, O. C., Tinoco, I., Brody, E. N., & Gold, L. (1988) *Proc. Natl. Acad. Sci. U.S.A. 85*, 1364–1368.
Vermote, C. L. M., & Halford, S. E. (1992) *Biochemistry 31*, 6082–6089.